

# 行政院國家科學委員會專題研究計畫 期末報告

探討磷脂醯肌醇三激?抑制劑在 Anti-Thy-1 抗體引發腎絲  
球腎炎動物模式中的抗發炎功能

計畫類別：個別型

計畫編號：NSC 101-2314-B-040-004-

執行期間：101年08月01日至102年07月31日

執行單位：中山醫學大學生物醫學科學學系(所)

計畫主持人：林庭慧

計畫參與人員：碩士級-專任助理人員：吳星佑

公開資訊：本計畫涉及專利或其他智慧財產權，2年後可公開查詢

中華民國 102年10月30日

中文摘要： 中文摘要

馬兜鈴酸 (AA) 是中草藥腎病的常見原因。馬兜鈴酸腎病 (AAN) 的發病機制中涉及的機制是複雜的。有證據顯示馬兜鈴酸 (AA) 造成腎臟纖維化。一氧化氮 (NO) 是一氧化氮合酶 (NOS) 經由催化 L-精氨酸產生之訊號傳遞氣體。一氧化氮 (NO) 參與腎血流動力學並對腎臟損傷的細胞具有保護作用。一氧化氮 (NO) 在 AA 腎病 (AAN) 扮演角色並不清楚。在本研究中，利用了 MES-13 細胞 (腎小球系膜細胞)，探討一氧化氮 (NO) 在馬兜鈴酸腎病 (AAN) 扮演的角色。由脂多醣 (LPS) 及干擾素 (IFN- $\gamma$ ) 刺激 MES-13 細胞，可刺激誘導型一氧化氮合酶 (iNOS) 的表現且產生內源性的一氧化氮 (NO)，而此內源性的一氧化氮 (NO) 可顯著下調結締組織生長因子 (CTGF) 蛋白質之表達。馬兜鈴酸 (AA) 顯著抑制 LPS / IFN- $\gamma$  誘導 NO 的產生並扭轉由 LPS / IFN- $\gamma$  下調之 CTGF 表達。馬兜鈴酸 (AA) 降低 iNOS 基因和蛋白質的表達，呈現濃度依賴的方式。馬兜鈴酸 (AA) 減弱 LPS / IFN- $\gamma$  誘導的信號轉導和激活轉錄-1 $\alpha$  (STAT-1 $\alpha$ ) 的磷酸化和干擾素反應因子 1 (IRF-1) 的 mRNA 的表達。此外，馬兜鈴酸 (AA) 降低 IKK 的磷酸化和降低 NF- $\kappa$ B 移位到細胞核。綜上所述，我們的結果顯示，馬兜鈴酸 (AA) 於 MES-13 細胞藉由抑制 NO 和 iNOS 的表達，逆轉 CTGF 表達，主要藉由抑制 JAK/STAT-1 $\alpha$  和 NF- $\kappa$ B 信號路徑。NO 藉由下調 CTGF 可發揮抗纖維化的作用。而馬兜鈴酸 (AA) 藉由抑制 iNOS 基因和蛋白質的表達及逆轉 CTGF 表達，或可作為馬兜鈴酸 (AA) 造成腎病纖維化可能機轉部分解釋。

中文關鍵詞： 關鍵詞：一氧化氮 (NO)；馬兜鈴酸 (AA)；結締組織生長因子 (CTGF)；腎小球系膜細胞 (MES-13 cells)。

英文摘要： Aristolochic acid (AA) is a common cause of Chinese herb nephropathy. The mechanisms involved in the pathogenesis of AA nephropathy (AAN) are intricate. One well-documented effect of AA in the kidney is its pro-fibrotic activity. Nitric oxide (NO), a messenger gas generated from L-arginine, is the product of nitric oxide synthase (NOS). NO is involved in renal hemodynamics and exerts cytoprotective effects

against renal injury. In the present study, the role of NO in AAN was investigated in MES-13 cells, a glomerular mesangial cell line. NO endogenously generated by the induction of inducible nitric oxide synthase (iNOS) with lipopolysaccharide (LPS)/interferon- $\gamma$  (IFN $\gamma$ ) significantly downregulated connective tissue growth factor (CTGF) protein expression in MES-13 cells. AA significantly suppressed LPS/IFN- $\gamma$ -induced NO production and reversed CTGF expression that was downregulated by LPS/IFN- $\gamma$ . AA decreased iNOS gene and protein expressions in a concentration-dependent manner. AA caused declines in LPS/IFN- $\gamma$ -induced signal transducer and activator of transcription-1 $\alpha$  (STAT-1 $\alpha$ ) phosphorylation and interferon response factor-1 (IRF-1) mRNA expression. Furthermore, AA attenuated I $\kappa$ B phosphorylation and reduced NF- $\kappa$ B translocation to the nuclear fraction. Taken together, our data indicate that AA reversed the CTGF expression inhibited by LPS/IFN- $\gamma$  treatment via suppression of NO and iNOS expressions in MES-13 cells through inhibition of the JAK/STAT-1 $\alpha$  and NF- $\kappa$ B signaling pathways. NO potentially exerts antifibrotic activity by down regulation of CTGF in MES-13 cells and inhibition of the iNOS gene by AA might partially account for the fibrotic effects of AA in nephropathy.

英文關鍵詞： Keywords: nitric oxide ; aristolochic acid ; connective tissue growth factor ; glomerular mesangial cells.

行政院國家科學委員會補助專題研究  
計畫

期中進度  
報告  
 期末報告

(計畫名稱)

探討磷脂醯肌醇三激酶抑制劑在 Anti-Thy-1 抗體引發腎絲球腎炎動物模式中的抗發炎功能

計畫類別： 個別型計畫  整合型計畫

計畫編號：NSC 101-2314-B-040-004-

執行期間：101年8月1日至102年7月31日

執行機構及系所：中山醫學大學生物醫學科學學系

計畫主持人：林庭慧

共同主持人：

計畫參與人員：吳星佑

本計畫除繳交成果報告外，另含下列出國報告，共 \_\_\_\_ 份：

- 移地研究心得報告
- 出席國際學術會議心得報告
- 國際合作研究計畫國外研究報告

處理方式：除列管計畫及下列情形者外，得立即公開查詢

涉及專利或其他智慧財產權， 一年  二年後可公開查詢

中華民國 102 年 10 月 30 日

## 國科會補助專題研究計畫成果報告自評表

請就研究內容與原計畫相符程度、達成預期目標情況、研究成果之學術或應用價值（簡要敘述成果所代表之意義、價值、影響或進一步發展之可能性）、是否適合在學術期刊發表或申請專利、主要發現或其他有關價值等，作一綜合評估。

1. 請就研究內容與原計畫相符程度、達成預期目標情況作一綜合評估

- 達成目標
- 未達成目標（請說明，以 100 字為限）
- 實驗失敗
- 因故實驗中斷
- 其他原因

說明：原本研究計畫所提之實驗設計，其實驗結果不如預期。因此，於計畫執行中期，修改實驗目標。本份成果報告之研究內容與原計畫仍有一定程度相關，即討論一氧化氮及其調控之相關訊息傳遞路徑對腎臟疾病之影響。

2. 研究成果在學術期刊發表或申請專利等情形：

- 論文：已發表 未發表之文稿 撰寫中 無
- 專利：已獲得 申請中 無
- 技轉：已技轉 洽談中 無
- 其他：（以 100 字為限）

3. 請依學術成就、技術創新、社會影響等方面，評估研究成果之學術或應用價值（簡要敘述成果所代表之意義、價值、影響或進一步發展之可能性）（以 500 字為限）

一些研究報告指出馬兜鈴酸 Aristolochic acid (AA)可減弱一個調節免疫反應主要的轉錄因子，NF- $\kappa$ B，之激活。然而，在這些論文中並沒有闡明此發現的生理意義。在這篇報告中，我們發現在腎臟絲球體細胞 MES-13 細胞中，馬兜鈴酸 Aristolochic acid (AA)可減弱 NF- $\kappa$ B 下游其靶基因之一：誘導型一氧化氮合酶 (iNOS) 之表現。最有趣的是，我們證明，LPS / IFN- $\gamma$  誘導內源性一氧化氮 (Nitric Oxide, NO) 的產生，並可下調結締組織生長因子 connective tissue growth factor (CTGF) 在 MES-13 細胞中之表現。CTGF 是腎臟纖維化之主要指

標蛋白質。Aristolochic acid (AA)顯著抑制由 LPS / IFN -  $\gamma$  誘導內源性一氧化氮(NO)的產生，並扭轉由一氧化氮 (NO)下調的 CTGF 表達。Aristolochic acid (AA)下調 iNOS 基因及逆轉由一氧化氮 (NO)下調的 CTGF 表達藉由 JAK/STAT-1  $\alpha$  和 NF- $\kappa$ B 訊息路徑。我們的結果顯示 Aristolochic acid (AA)可減弱 NF- $\kappa$ B，下調 iNOS 基因，逆轉由一氧化氮 (NO)下調的 CTGF 蛋白質表達。這些結果或可部分解釋一些馬兜鈴屬植物具有造成腎臟纖維化之能力。此份研究報告提供馬兜鈴酸腎病之可能致病機轉及提供馬兜鈴酸腎病之治療策略。

## (二)中、英文摘要及關鍵詞 (keywords)。

### 中文摘要

馬兜鈴酸 (AA) 是中草藥腎病的常見原因。馬兜鈴酸腎病 (AAN) 的發病機制中涉及的機制是複雜的。有證據顯示馬兜鈴酸(AA)造成腎臟纖維化。一氧化氮(NO) 是一氧化氮合酶(NOS)經由催化L-精氨酸產生的訊號傳遞氣體。一氧化氮(NO) 參與腎血流動力學並對腎臟損傷的細胞具有保護作用。一氧化氮(NO) 在 AA 腎病 (AAN) 扮演角色並不清楚。在本研究中，利用了MES-13細胞(腎小球系膜細胞)，探討一氧化氮(NO) 在馬兜鈴酸腎病 (AAN) 扮演的角色。由脂多醣(LPS) 及干擾素 (IFN- $\gamma$ ) 刺激MES-13細胞，可刺激誘導型一氧化氮合酶(iNOS)的表現且產生內源性的一氧化氮(NO)，而此內源性的一氧化氮(NO) 可顯著下調結締組織生長因子(CTGF)蛋白質之表達。馬兜鈴酸(AA)顯著抑制LPS / IFN- $\gamma$ 誘導NO的產生並扭轉由LPS / IFN- $\gamma$ 下調之CTGF表達。馬兜鈴酸(AA)降低iNOS基因和蛋白質的表達，呈現濃度依賴的方式。馬兜鈴酸(AA)減弱LPS / IFN- $\gamma$ 誘導的信號轉導和激活轉錄-1 $\alpha$  (STAT-1 $\alpha$ )的磷酸化和干擾素反應因子1 (IRF-1)的mRNA的表達。此外，馬兜鈴酸(AA)降低IKB的磷酸化和降低NF- $\kappa$ B移位到細胞核。綜上所述，我們的結果顯示，馬兜鈴酸(AA)於MES-13細胞藉由抑制NO和iNOS的表達，逆轉CTGF表達，主要藉由抑制JAK/STAT-1 $\alpha$ 和NF- $\kappa$ B信號路徑。NO藉由下調CTGF可發揮抗纖維化的作用。而馬兜鈴酸(AA)藉由抑制iNOS基因和蛋白質的表達及逆轉CTGF表達，或可作為馬兜鈴酸(AA)造成腎病纖維化可能機轉部分解釋。

關鍵詞：一氧化氮(NO)；馬兜鈴酸(AA)；結締組織生長因子(CTGF)；腎小球系膜細胞(MES-13 cells)。

## 英文摘要

### **Abstract**

Aristolochic acid (AA) is a common cause of Chinese herb nephropathy. The mechanisms involved in the pathogenesis of AA nephropathy (AAN) are intricate. One well-documented effect of AA in the kidney is its pro-fibrotic activity. Nitric oxide (NO), a messenger gas generated from L-arginine, is the product of nitric oxide synthase (NOS). NO is involved in renal hemodynamics and exerts cytoprotective effects against renal injury. In the present study, the role of NO in AAN was investigated in MES-13 cells, a glomerular mesangial cell line. NO endogenously generated by the induction of inducible nitric oxide synthase (iNOS) with lipopolysaccharide (LPS)/interferon- $\gamma$  (IFN $\gamma$ ) significantly downregulated connective tissue growth factor (CTGF) protein expression in MES-13 cells. AA significantly suppressed LPS/IFN- $\gamma$ -induced NO production and reversed CTGF expression that was downregulated by LPS/IFN- $\gamma$ . AA decreased iNOS gene and protein expressions in a concentration-dependent manner. AA caused declines in LPS/IFN- $\gamma$ -induced signal transducer and activator of transcription-1 $\alpha$  (STAT-1 $\alpha$ ) phosphorylation and interferon response factor-1 (IRF-1) mRNA expression. Furthermore, AA attenuated I $\kappa$ B phosphorylation and reduced NF- $\kappa$ B translocation to the nuclear fraction. Taken together, our data indicate that AA reversed the CTGF expression inhibited by LPS/IFN- $\gamma$  treatment via suppression of NO and iNOS expressions in MES-13 cells through inhibition of the JAK/STAT-1 $\alpha$  and NF- $\kappa$ B signaling pathways. NO potentially exerts antifibrotic activity by down regulation of CTGF in MES-13 cells and inhibition of the *iNOS* gene by AA might partially account for the fibrotic effects of AA in nephropathy.

Keywords: nitric oxide; aristolochic acid; connective tissue growth factor; glomerular mesangial cells.



## 目錄

1. 前言 Introduction
2. 研究方法 Materials and Methods
  - 2.1. Materials.
  - 2.2. Cell Culture.
  - 2.3. Nitrite Assay.
  - 2.4. Preparation of Whole Cell Extract and Western Blot Analysis.
  - 2.5. Preparation of Cytosolic and Nuclear Extracts.
  - 2.6. Reverse Transcription Polymerase Chain Reaction (RT-PCR).
  - 2.7. Real-Time RT-PCR
  - 2.8. Electrophoretic Mobility Shift Assay (EMSA).
  - 2.9. Statistical Analysis.
3. 結果 (Results)
  - 3.1. NO endogenously generated by the induction of iNOS with LPS/IFN- $\gamma$  significantly downregulated the protein expression of CTGF in AA-treated MES-13 cells.
  - 3.2. AA suppressed nitrite production in LPS/IFN- $\gamma$ -stimulated MES-13 cells.
  - 3.3. AA inhibited iNOS protein expression and reversed the CTGF protein expression that was downregulated by LPS/IFN- $\gamma$  treatment in MES-13 cells.
  - 3.4. AA decreased iNOS mRNA levels in LPS/IFN- $\gamma$ -stimulated culture.
  - 3.5. Effects of AA on LPS/IFN- $\gamma$ -modulated STAT-1 $\alpha$  phosphorylation.
  - 3.6. AA reduced IRF-1 protein expression.
  - 3.7. The presence of AA prevented the nuclear translocation of NF- $\kappa$ B and phosphorylation of I $\kappa$ B.
4. 討論 (Discussion)
5. 附圖 (Figures)
6. 參考文獻 (References)

(三)報告內容：包括前言、研究目的、文獻探討、研究方法、結果與討論（含結論與建議）等。

## 1. Introduction

Nitric oxide (NO) is a labile radical gas that exhibits a broad range of functions in biology [1-3]. NO is formed from L-arginine by three NO synthases (NOSs) including inducible (i)NOS, neuronal (n)NOS, and endothelial (e)NOS [1-3]. NO signaling is primarily mediated by cGMP, which is synthesized by NO-activated guanylyl cyclases and broken down by cyclic nucleotide phosphodiesterases (PDEs) [1-3]. In cGMP-independent mechanisms, NO either reacts with oxygen and superoxide radicals to form peroxynitrite or modifies the target protein through S-nitrosylation of cysteine thiol residues, which appear to be emerging mechanisms of NO signaling in diverse functions [1-3]. NO is involved in a variety of physiological processes in the kidney, including mediating tubular ion transport, regulating extracellular fluid volume, renin release and exerting cytoprotective effects against renal injury [4]. Under pathophysiologic conditions, NO is involved in renal hypertension, immune-mediated glomerulonephritis, glomerulosclerosis, interstitial fibrosis, diabetic nephropathy and transplant rejection [4].

Aristolochic acid (AA) produced from *Artislochia fangchi* is a common cause of Chinese herb nephropathy (CHN) and Balkan endemic nephropathy [5]. AA-induced nephropathies (AAN) are associated with urothelial cancer development through AA-specific DNA adducts [6]. Patients with AAN show a rapidly progressive decline in renal function, resulting in end-stage renal failure requiring hemodialysis [7]. Pathologically, AAN is associated with tubular atrophy, severe anemia, inflammation and cortical interstitial fibrosis with interstitial nephritis [8]. The mechanisms involved in the pathogenesis of AAN are complicated and remain to be investigated.

Connective tissue growth factor (CTGF) is a secreted protein comprised of four conserved cysteine residue-rich domains [9]. Each functional domain has the capacity to interact with multiple biological ligands, such as growth factors, cell surface

receptors and extracellular matrix proteins [9]. CTGF mediates the stimulatory actions of transformation growth factor  $\beta$  (TGF $\beta$ ) on extracellular matrix accumulation (ECM) synthesis and is strongly upregulated in fibrotic tissue [10]. CTGF is a key factor in the onset and progression of kidney damage and is involved in several forms of nephropathy [11, 12]. CTGF might be a potential therapeutic target for AAN.

The overall production of NO is reduced in chronic kidney disease (CKD) [13]. Pharmacologic intervention by replenishing NO production has been used to lessen the complications of CKD [13]. The protective role of NO in renal injury has been reported in several animal models of renal disease [14]. Due to the meager information regarding the role of NO in AAN, whether NO exhibits antifibrotic effects in AAN and the underlying mechanisms were investigated in MES-13 cells in this study.

In the present study, we demonstrate that NO endogenously generated by iNOS downregulated CTGF expression in MES-13 cells. AA significantly suppressed LPS/IFN- $\gamma$ -induced NO production and reversed the CTGF expression that was downregulated by iNOS. We further demonstrate that AA inhibited LPS/IFN- $\gamma$ -stimulated NO production in MES-13 cells via JAK/STAT-1 $\alpha$  and NF- $\kappa$ B pathways. Our data indicate that the downregulation of *iNOS* gene by AA might partially account for the pro-fibrogenic activity of some plants from the genus *Aristolochia*.

## **2. Materials and Methods**

### **2.1. Materials.**

Fetal bovine serum was from Highclon (Logan, UT). DMEM medium and Ham's F12 medium and medium supplements were obtained from Gibco BRL (Gaithersburg, MD). LPS and AA were obtained from Sigma Chemical Company (St. Louis, MO). IFN- $\gamma$  was purchased from PeproTech EC Ltd. (London, UK). The specific antibodies for iNOS, CTGF, glyceraldehyde-3-phosphate dehydrogenase (GAPDH), inhibitor  $\kappa$ B $\alpha$  (I $\kappa$ B $\alpha$ ) and IRF-1 were products from Santa Cruz Biotechnology (Santa Cruz, CA). Antibody for p65 (NF- $\kappa$ B) was acquired from BD Biosciences (Franklin Lakes, NJ). Phosphorylated STAT-1 $\alpha$ , STAT-1 $\alpha$ ,

phosphorylated I $\kappa$ B $\alpha$  antibodies were purchased from Cell Signaling Technology Inc.(Beverly, MA). Oligonucleotide primer sequences of iNOS, IRF-1 and GAPDH for reverse-transcriptase polymerase chain reaction (RT-PCR) and quantitative real-time reverse transcription polymerase chain reaction (Q-RT-PCR) were selected by using Primer Select (MD Bio, Inc). The nylon membranes (Hybond N<sup>+</sup>) for electrophoretic mobility shift assay (EMSA) were purchased from Amersham Pharmacia Biotech Inc., (Piscataway, NJ). PGE<sub>2</sub> EIA kit was purchased from Cayman Chemical Company (Ann Arbor, Michigan).

## 2.2. Cell Culture.

The MES-13 cell line (glomerular mesangial cells from an SV40 transgenic mouse) was obtained from American Type Culture Collection (CRL-1927; Manassas, VA, USA) and maintained in culture medium with a 3:1 mixture of DMEM medium and Ham's medium, supplemented with 14 mM HEPES, 2 mM glutamine, antibiotics (100  $\mu$ g/ml penicillin and 100  $\mu$ g/ml streptomycin) and 5 % fetal bovine serum at 37<sup>0</sup> C. The incubation chamber was equilibrated with 5% CO<sub>2</sub>- 95% air.

## 2.3. Nitrite Assay.

Nitrite assay was performed to measure NO production in MES-13 cells after different treatment. NO is rapidly converted into nitrite as the end product. Thus, the nitrite accumulation in culture supernatant was used as indirect measures of the amount of NO produced. The Griess assay [15] was used and the nitrite level was measured in triplicate. Briefly, an aliquot of 100  $\mu$ l of the culture supernatant of MES-13 cells was mixed with 100  $\mu$ l of Griess reagent (one part 0.1% N -(1-naphtyl) ethylene-diamine dihydrochloride in water and one part 1% sulfanilamide in 5% H<sub>3</sub>PO<sub>4</sub>; both purchased from Sigma Chemicals). The mixture was incubated for ten minutes at room temperature in the dark. The absorbance at 540 nm was measured and the nitrite concentration was calculated by comparison to standard curves of sodium nitrite in culture medium.

## 2.4. Preparation of Whole Cell Extract and Western Blot Analysis.

To detect the protein levels of iNOS and CTGF after exposure to different stimuli, MES-13 cells were washed with 1x PBS, scraped out, and incubated with

lysis buffer. The lysis buffer contained 1x PBS, 1% Nonidet P-40, 0.5% sodium deoxycholate, 0.1% SDS and protease inhibitor cocktail tablet (Roche Applied Science, Mannheim, Germany). Cells suspended in lysis buffer were sonicated. The homogenate was centrifuged at 13,000 rpm for 40 min at 4°C, and the cell supernatant was collected. The protein concentration was measured using a Bio-Rad protein assay kit. Cell lysate was combined with 5 x sample buffer containing 100 mM Tris-HCl (pH 6.8), 20% glycerol, 7% SDS, 5% mercaptoethanol, and 0.1% bromophenol blue. The sample was boiled for 5 min and centrifuged to remove the debris. Equal amounts of protein samples (60 µg) were subjected to SDS-PAGE using 10% polyacrylamide gels. Following electrophoresis, the gel was transferred to a polyvinylidene difluoride (PVDF) membrane, blocked with 5% skim-milk in Tris-buffered saline (TBS) containing 10 mM Tris (pH 8.0) and 150 mM NaCl, then incubated with primary antibody at 4°C overnight. TBS containing 0.02% Tween 20 (TBST) was used to wash out the nonspecific binding material on the PVDF membrane. Finally, the membrane was incubated with secondary antibody for 1 h at room temperature. After washing with TBST, the immunoreactive bands were visualized with a light-emitting kit (ECL, Amersham, UK). The protein amount was quantified by measuring the area of the iNOS and CTGF bands using densitometric analysis with AlphaEaseFC.

## 2.5. Preparation of Cytosolic and Nuclear Extracts.

To determine cytoplasmic IκB phosphorylation and nuclear NF-κB protein level, cytoplasmic and nuclear proteins of MES-13 cells were prepared using NE-PER nuclear and cytoplasmic extraction reagents (Pierce Chemical Company, Rockford, IL) containing proteinase inhibitors cocktail. Phosphorylation of IκB in cytoplasmic extracts and activation of NF-κB in nuclear extracts were analyzed by Western blot. The primary antibodies for phosphorylated IκB and NF-κB p65 were purchased from Cell Signaling Technology, Inc. (Beverly, MA) and Santa Cruz Biotechnology (Santa Cruz, CA), respectively. STAT-1α phosphorylation was also determined. The primary antibodies for detection of STAT-1α protein and phosphorylation were purchased from Cell Signaling Technology, Inc. (Beverly, MA).

## 2.6. Reverse Transcription Polymerase Chain Reaction (RT-PCR).

Total RNA was isolated from MES-13 cells using the Tri reagent RNA isolation reagent (Molecular Research Center, Inc, Cincinnati, OH, USA). Total RNA was reverse transcribed to cDNA using Superscript II reverse transcription RT-PCR kit (Life Technologies, Gaithersburg, MD) followed by amplification with PCR. The oligonucleotide primers for the RT-PCR were as followed:  
5'-CAGTTCTGCGCCTTTGCTCAT-3' (forward) and  
5'-GGTGGTGCGGCTGGACTTT-3'(reverse) for iNOS;  
5'-CGATACAAAGCAGGGGAAAA-3' (forward) and  
5'- TAGCTGCTGTGGTCATCAGG-3' (reverse) for IRF-1 and  
5'- CATCATCTCCGCCCTTCT-3 (forward) and  
5'-CTCGTGGTTCACACCCATCA-3 (reverse) for GAPDH. After an initial denaturation at 94 °C for 3 min, 35 cycles of amplification (94°C for 30 sec, 58.3°C for 30 sec , and 72 °C for 1 min) were performed followed by a 7 min extension at 72<sup>0</sup>C for iNOS; an initial denaturation at 94 °C for 3 min, 31 cycles of amplification (94°C for 30 sec, 50°C for 30 sec , and 72 °C for 1 min) were performed followed by a 7 min extension at 72<sup>0</sup>C for IRF-1; an initial denaturation at 94 °C for 3 min, 40 cycles of amplification (94°C for 30 sec, 60°C for 30 sec, and 72 °C for 1 min) were performed followed by a 7 min extension at 72<sup>0</sup>C for GAPDH. The amplified PCR products were analyzed on a 1 % agarose gel. The PCR product of GAPDH was used as an internal control for quantitation.

## 2.7. Real-Time RT-PCR

Total cellular RNA was extracted from MES-13 cells using Tri reagent RNA isolation reagent (Molecular Research Center, Inc., Cincinnati, OH, USA). The cDNAs were synthesized from 3.5 µg of RNA of each sample using a SuperScript<sup>TM</sup> II reverse transcription system kit according to the manufacturer's protocol. The primers used were as followed: 5'-CCGATTTAGAGTCTTGGTGAAAGTG -3' (forward) and 5'-TGACCCGTGAAGCCATGA-3' (reverse) for iNOS;  
5'-CCGATACAAAGCAGGAGAAAAAG -3' (forward) and  
5'- TGGCACAACGGAAGTTTGC -3' (reverse) for IRF-1;  
5'-CATCATCTCCGCCCTTCT-3' (forward),  
5'-CTCGTGGTTCACACCCATCA-3' (reverse) for GAPDH. The Q-RT-PCR was carried out in a 25 µl final volume containing: 3 µg cDNA sample, 500 nM primer

pairs and 12.5  $\mu$ l SYBR Green PCR Master Mix, and performed by an initial denaturation at 95°C for 10 min, followed by 40 cycles of amplification at 95°C for 15 sec and 60°C for 60 sec in an ABI PRISM 7000 system sequence detector (Applied Biosystems). Each RNA sample was measured in duplication. The specificity of amplified PCR products was evaluated by a comparative Ct method. The threshold cycle value (Ct value), which is inversely proportional to the initial template copy number, is calculated from cycle number at which the PCR product crosses a threshold of detection. The iNOS (or IRF-1) mRNA expression were normalized against GAPDH and gene expression changes induced by various treatments were determined by the  $2^{-\Delta\Delta CT}$  method.

## 2.8. Electrophoretic Mobility Shift Assay (EMSA).

MES-13 cells were pre-treated with AA (40  $\mu$ M and 50  $\mu$ M) for 12 hr, followed by stimulation with 1  $\mu$ g/ml LPS and 10 ng/ml IFN- $\gamma$  for 40 min. Thereafter, nuclear extracts were prepared by NE-PER nuclear and cytoplasmic extraction reagents (Pierce Chemical Company) and stored at 4°C until the EMSA was performed. The LightShift Chemiluminescent EMSA Kit was purchased from Pierce Chemical Co. The biotin-labeled and unlabeled oligonucleotides, corresponding to the NF- $\kappa$ B binding sites were synthesized. The sequences utilized were as followed: 5'-AGTTGAGGGGACTTTCCCAGGC-3' (for NF- $\kappa$ B). Nuclear extract (10  $\mu$ g), poly (dI-dC), and biotin-labeled probes were mixed with the binding buffer (to a final volume of 20  $\mu$ l) and were incubated at room temperature for 30 min. The nuclear protein-DNA complex was separated by a native 6% polyacrylamide gel electrophoresis and then transferred to nylon membranes (Hybond N<sup>+</sup>). Next, the membrane was treated with streptavidin-horseradish peroxidase, and the nuclear protein-DNA bands were developed with the use of a SuperSignal West Pico kit (Pierce Chemical Co).

## 2.9. Statistical Analysis.

The values were expressed as the mean  $\pm$  SEM of at least three independent experiments. Data were analyzed by one-way analysis of variance (ANOVA) followed by either the Bonferroni's or the Dunnett's method for multi-group comparison tests. A value of  $p < 0.05$  was considered as statistical significantly.

### 3. Results

3.1. NO endogenously generated by the induction of iNOS with LPS/IFN- $\gamma$  significantly downregulated the protein expression of CTGF in AA-treated MES-13 cells.

To investigate the role of NO in AAN, the effect of NO on CTGF protein expression was investigated. As shown in Fig. 1, A-C (lane 1, control), CTGF protein was detectable in MES-13 cells cultured with medium only. NO endogenously generated by the induction of iNOS with LPS/IFN- $\gamma$  inhibited CTGF protein expression in MES-13 cells. A significant reduction in CTGF protein expression was observed in several independent studies, as shown in Fig. 1 (A-C, lanes 1 and 2). CTGF protein expression was slightly increased when treated with different concentration of AA at doses of 30, 40, and 50  $\mu$ M (Fig. 1, A-C, lane 3). The treatment of MES-13 cells with AA alone did not trigger iNOS protein expression or NO production (data not shown). Most importantly, AA significantly suppressed LPS/IFN- $\gamma$ -induced NO production (Fig. 2) and reversed CTGF protein expression that was downregulated by LPS/IFN- $\gamma$  (Fig. 1, A-C, lanes 2 and 4).

3.2. AA suppressed nitrite production in LPS/IFN- $\gamma$ -stimulated MES-13 cells.

MES-13 cells were co-treated with various concentrations of AA (20, 30, 40, and 50  $\mu$ M) for 24 h in the presence of LPS/IFN- $\gamma$ . The cell medium was collected, and nitrite concentrations within the medium were determined by a Griess assay. Exposure of cells to LPS/IFN- $\gamma$  resulted in nitrite release to  $32.42 \pm 3.7$   $\mu$ M. AA doses of 20, 30, 40, and 50  $\mu$ M significantly modulated levels of nitrite to  $31.18 \pm 4.0$ ,  $25.92 \pm 3.7$ ,  $20.38 \pm 1.8$ , and  $12.32 \pm 2.1$   $\mu$ M, respectively. Nitrite levels were reduced by over 20%, 40%, and 60% upon treatment with AA at doses of 30, 40, and 50  $\mu$ M, in that order (Fig.2). These results indicate that the inhibitory effect of AA on LPS/IFN- $\gamma$ -triggered nitrite production in MES-13 cells was in a concentration-dependent manner.

3.3. AA inhibited iNOS protein expression and reversed the CTGF protein expression that was downregulated by LPS/IFN- $\gamma$  treatment in MES-13 cells.

The expression of iNOS protein in treated MES-13 cells was determined by Western blotting. As shown in Fig. 3, the iNOS protein level markedly increased in cultures treated with a combination of LPS and IFN- $\gamma$ . The addition of AA reduced the expression of stimulated iNOS protein in a concentration-dependent way. The value of LPS/IFN- $\gamma$ -induced iNOS protein as control level was set as 100 %.The



signals of iNOS protein significantly decreased to 71%, 50% and 44% of the control level following treatment with 30, 40, and 50  $\mu$ M of AA, respectively. On the other hand, LPS, IFN- $\gamma$  or AA alone did not modulate expression levels of iNOS protein (data not shown). These results suggest that the inhibitory effect of AA on LPS/IFN- $\gamma$ -stimulated NO production was accompanied by reduced expression of iNOS protein. Most notably, also shown in Fig. 3, the CTGF protein expression that was downregulated by LPS/IFN- $\gamma$  was reversed with the treatment of increasing concentrations of AA at 30, 40, and 50  $\mu$ M. These results confirm that NO endogenously generated by the induction of iNOS with LPS/IFN- $\gamma$  significantly downregulates the protein expression of CTGF and the inhibitory effect of AA on NO reversed the CTGF protein expression in MES-13 cells.

#### 3.4. AA decreased iNOS mRNA levels in LPS/IFN- $\gamma$ -stimulated culture.

To examine whether the inhibitory action of AA on LPS/IFN- $\gamma$ -stimulated NO production is correlated with the iNOS gene expression at transcriptional level, semiquantitative RT-PCR and real-time RT-PCR were performed to determine the iNOS mRNA level in MES-13 cells. MES-13 cells were treated with an LPS and IFN- $\gamma$  mixture in the absence or presence of various concentrations of AA (20, 30, 40, and 50  $\mu$ M). As revealed by a semiquantitative RT-PCR in Fig. 4A, signals of iNOS mRNA gradually diminished with increasing concentrations of AA. Similar inhibitory effects of AA were detected by quantitative real-time RT-PCR. The presence of 30, 40, and 50  $\mu$ M AA inhibited levels of LPS/IFN- $\gamma$ -stimulated iNOS mRNA to 61%, 55% and 33% of the control level, respectively (Fig.4B). These data indicate that the inhibitory effects of AA on LPS/IFN- $\gamma$ -stimulated NO production occurred at the transcriptional regulation of iNOS gene expression.

#### 3.5. Effects of AA on LPS/IFN- $\gamma$ -modulated STAT-1 $\alpha$ phosphorylation.

To investigate whether AA attenuates transcriptional expression of the iNOS gene through interrupting the upstream signaling of iNOS gene, we first elucidated the effect of AA on activation of the JAK/STAT-1 $\alpha$  pathway; tyrosine phosphorylation (Tyr701) of STAT-1 $\alpha$  indicated the prime effect of IFN- $\gamma$  on iNOS gene expression [16]. MES-13 cells were pre-incubated with or without AA for 12 h and then treated with LPS/IFN- $\gamma$  for another 3 h. Cytoplasmic and nuclear fractions of

MES-13 cells were separately collected and applied to Western blotting to examine STAT-1 $\alpha$  phosphorylation. In Fig. 5A, upon treatment of cultures with LPS/IFN- $\gamma$ , a strikingly high level of phospho-STAT-1 $\alpha$  was observed in the nuclear fraction of MES-13 cells. Co-incubation with 40 and 50  $\mu$ M AA led to a significant attenuation of STAT-1 $\alpha$  phosphorylation induced by LPS/IFN- $\gamma$ . This result indicated that AA exerts its inhibitory action on LPS/IFN- $\gamma$ -triggered iNOS gene expression through suppression of the STAT-1 $\alpha$  signaling pathway. However, neither AA nor LPS/IFN- $\gamma$  alone changed the levels of phosphorylated STAT-1 $\alpha$  in the cytoplasmic fraction (data not shown).

### 3.6. AA reduced IRF-1 protein expression.

IRF-1 is one of the target genes of phosphorylated STAT-1 $\alpha$  and is able to bind with IREs located in the 5'-flanking region of the murine iNOS gene [17, 18]. To further confirm that suppression of STAT-1 $\alpha$  phosphorylation by AA can lead to an ineffective response of its target gene, the effect of AA on IRF-1 expression was investigated. Levels of the IRF-1 transcript were faintly detected by a real-time RT-PCR in unstimulated MES-13 cells. Stimulation of MES-13 cells with LPS/IFN- $\gamma$  enhanced IRF-1 mRNA expression while co-supplementation of AA reversed this effect (data not shown). A similar result was observed in IRF-1 protein levels in LPS/IFN- $\gamma$ -stimulated MES-13 cells (Fig.5B). After treatment of cultures with 40 and 50  $\mu$ M AA, signals of the IRF-1 protein decreased to 80% and 53% of LPS/IFN- $\gamma$ -stimulated cells, respectively.

### 3.7. The presence of AA prevented the nuclear translocation of NF- $\kappa$ B and phosphorylation of I $\kappa$ B.

Both NF- $\kappa$ B and STAT-1 $\alpha$  were reported to modulate iNOS gene expression in cell- and species-specific manners [19]. To further explore the mechanism underlying the inhibitory effect of AA on iNOS gene transcription, levels of NF- $\kappa$ B p65 in nuclear extracts were determined by Western blotting. As shown in Fig. 6A, the nuclear translocation of p65 was observed after the addition of LPS/IFN- $\gamma$  to MES-13 cells. In addition, the presence of AA (40 and 50  $\mu$ M) significantly blocked the nuclear translocation of p65 triggered by LPS/IFN- $\gamma$ .

To confirm the inhibitory effect of AA on suppressing NF- $\kappa$ B activation, we next performed EMSA to assess whether AA affected the binding of NF- $\kappa$ B to DNA *in vitro*. In LPS/IFN- $\gamma$ -activated MES-13 cells, a substantial increase in the DNA-binding activity of NF- $\kappa$ B was observed compared to untreated cells, but co-incubation with AA (40 and 50  $\mu$ M) led to a lower DNA-binding activity of NF- $\kappa$ B (Fig. 6B). The specificity of binding was assured by competition with the addition of excessive unlabelled oligonucleotides.

Moreover, phosphorylation of I $\kappa$ B, an upstream inhibitor of NF- $\kappa$ B, was examined. As shown in Fig. 7, phosphorylated I $\kappa$ B- $\alpha$  was barely detectable in resting MES-13 cells, but upon treatment with LPS/IFN- $\gamma$  for 20 min, I $\kappa$ B- $\alpha$  phosphorylation was strikingly initiated. Incubation of cultures with AA (40 and 50  $\mu$ M) for 12 h moderately suppressed I $\kappa$ B- $\alpha$  phosphorylation in MES-13 cells (Fig.7). Taken together, these results suggest that AA inhibited iNOS gene expression through suppression of NF- $\kappa$ B activation by blockade of I $\kappa$ B- $\alpha$  phosphorylation.

#### 4. Discussion

Plants of the genus *Aristolochia* have been used as anti-inflammatory drugs in traditional medicine. Conversely, the safety of using *Aristolochia fangchi* as botanical remedies has been denied because AA causes severe toxic effects, particularly to the kidneys and liver, and AAN is also complicated by a high risk of urothelial malignancy [5, 6]. The mechanisms involved in the pathogenesis of AAN are intricate. It is known that TGF-beta/Smad3 signaling is an essential mediator for chronic AAN [20], while the renin-angiotensin system is not involved in renal interstitial fibrosis induced by AA [21]. Moreover, CTGF, an important fibrogenic factor involved in stimulating fibronectin matrix synthesis, acts as a downstream mediator of TGF- $\beta$  in promoting fibrosis and is involved in AAN [10, 12]. Outlining the mechanisms that underlie regulation in AAN might help design potential therapeutic interventions for AA-induced kidney damage.

NO is a magic paracrine factor involved in versatile physiological and pathophysiological conditions. NO serves a protective role in preventing tissue fibrosis in the kidney, heart and liver because chronic administration of L-NAME, asymmetric dimethylarginine (ADMA), and FR260330 (all are iNOS inhibitors) leads to fibrosis of these organs [22, 23, 24, 25]. NO derived from iNOS act as an antifibrogenic defense mechanism in a rat model of Peyronie's disease (PD) [25]. In the kidney, treatment modalities that increase NO formation improve the tubulointerstitial fibrosis of obstructive nephropathy [26], while in iNOS-knocked mice, interstitial fibrosis of unilateral urethral obstruction is exacerbated [27]. In streptozocin (STZ) -induced diabetic mice, tubulointerstitial fibrosis was more evident in iNOS knockout mice than the wild type [28]. This indicates that iNOS-derived NO modulates glomerulosclerosis and tubulointerstitial fibrosis in chronic STZ diabetic nephropathy [28]. NO exerts antifibrotic activity by downregulation of fibrogenic factor [29, 30, 31]. NO acts as a strong repressor of CTGF expression in cultured rat mesangial cells and downregulates the expression of extracellular matrix genes linked to fibrosis [30,31]. These studies indicated that pharmacologic manipulations that increase NO might be advantageous to the obstructed kidneys. Whether NO exerts antifibrotic activity by down-regulation of CTGF in AAN and the underlying mechanisms have never been investigated.

In the present study, stimulation of MES-13 cells with LPS/IFN- $\gamma$  led to a significant decrease in CTGF protein expression in several independent studies (Fig. 1, A-C, lane 2). These indicate NO endogenously generated by the induction of iNOS with LPS/ IFN $\gamma$  significantly downregulated CTGF protein expression in MES-13

cells. Neither NO production nor iNOS protein expression was detectable in the presence of AA alone. The expression of iNOS protein in MES-13 cells was only induced by a combination of LPS and IFN- $\gamma$ . Nitrite levels in LPS/ IFN $\gamma$ -stimulated MES-13 cells were reduced by over 20%, 40%, and 60%, respectively with AA treatment at doses of 30, 40, and 50  $\mu$ M (Fig. 2). Interestingly, AA significantly suppressed LPS/IFN- $\gamma$ -induced NO production and reversed CTGF expression downregulated by LPS/IFN- $\gamma$ . Thus, through suppression of LPS/IFN- $\gamma$ -induced NO production, AA might exhibit pro-fibrogenic activity through upregulation of CTGF expression in MES-13 cells.

Coincident with the changes in NO production, AA dramatically decreased iNOS protein and mRNA expressions as shown in Figs. 3 and 4, respectively. These results suggested that attenuation of NO production by AA may in part stem from suppression of iNOS gene induction. It is known that LPS induces iNOS gene expression through activation of NF- $\kappa$ B, while IFN- $\gamma$  works through activation of STAT-1 $\alpha$ . By binding to the 5'-flanking regions of the *iNOS* gene, activated NF- $\kappa$ B and STAT-1 $\alpha$  work synergistically to elicit iNOS gene expression. We further identified whether AA reversed the IFN- $\gamma$ -elicited NO generation through preventing the phosphorylation of the STAT-1 $\alpha$  protein in MES-13 cells. As shown in Fig.5 (A), co-incubation with AA led to a significant attenuation of STAT-1 $\alpha$  phosphorylation induced by LPS/IFN- $\gamma$ . Moreover, as shown in Fig.5 (B), the presence of AA further downregulated expression of the *IRF-1* gene, a target gene of the STAT-1 $\alpha$  protein [32]. Both STAT-1 $\alpha$  and IRF-1 are transcriptional factors which bind to the GAS and IFN-stimulated regulatory elements (ISREs), respectively, and three copies of GAS and two copies of ISRE are located within the 1.7-kb fragment of the 5'-flanking region of the murine *iNOS* gene [17]. Therefore, AA, by inhibiting STAT-1 $\alpha$  activation, may play an important role in modulating antifibrotic activity of NO.

We also identified whether AA suppressed iNOS-dependent NO generation through inhibition of I $\kappa$ B phosphorylation and NF- $\kappa$ B DNA-binding activity (Fig.6 and Fig.7). These data suggest an immunosuppressive role of AA in transcriptional expression of the *iNOS* gene. NF- $\kappa$ B is regarded as a central mediator of the human immune response and regulates the transcription of various cytokine genes encoding IL-1 $\beta$ , IL-6, and TNF- $\alpha$  [33]. Within the promoter region of the murine iNOS gene, two NF- $\kappa$ B-binding sites are located at -961 and -76 base pairs, respectively [17]. Our data indicated that AA exerts its ability to block iNOS-derived NO synthesis through inhibition of NF- $\kappa$ B activation. In a recent report by Chen et al [34], they used a microarray analysis and demonstrated that incubation of normal human kidney HK-2

cells with AA inhibited NF- $\kappa$ B signaling. Moreover, AA inhibited TNF--induced MMP-9 in human monocytic THP-1 cells through blocking NF- $\kappa$ B activation [35]. Thus, combined with their data, we concluded that AA inhibits iNOS-dependent NO production by suppressing binding of NF- $\kappa$ B to the promoter region of the *iNOS* gene in MES-13 cells.

Vivancos and Moreno have reported PGE<sub>2</sub> via EP4 receptor/cAMP signaling was involved in NO release induced by LPS in macrophages RAW 264.7 cultures [36]. Since AA modulates PLA<sub>2</sub> activity and eicosanoid release [37, 38] and EP4 has been identified as the major PGE<sub>2</sub> receptor in MES-13 cells [39], we also investigated the effect of AA on PGE<sub>2</sub> production in MES-13 cells. The PGE<sub>2</sub> content after exposure of MES-13 cells with LPS/IFN $\gamma$  and AA at concentrations of 40 and 50  $\mu$ M were measured using PGE<sub>2</sub> EIA kit. No difference in PGE<sub>2</sub> release from MES-13 cells was observed after AA treatment. Thus, our data indicated the effect of AA on NO production was not caused by its effect on arachidonic acid cascade in MES-13 cells.

In summary, the present study demonstrated that AA reversed CTGF protein expression inhibited by LPS/IFN- $\gamma$  treatment via suppression of NO and iNOS expression in MES-13 cells by blocking the JAK/STAT-1 $\alpha$  and NF- $\kappa$ B signaling pathways. NO potentially enables antifibrotic activity by down regulation of CTGF in MES-13 cells, and downregulation of the *iNOS* gene by AA might partially explain the pro-fibrogenic activity effect of some plants from the *Aristolochia* in causing nephropathy.

**Figures.**

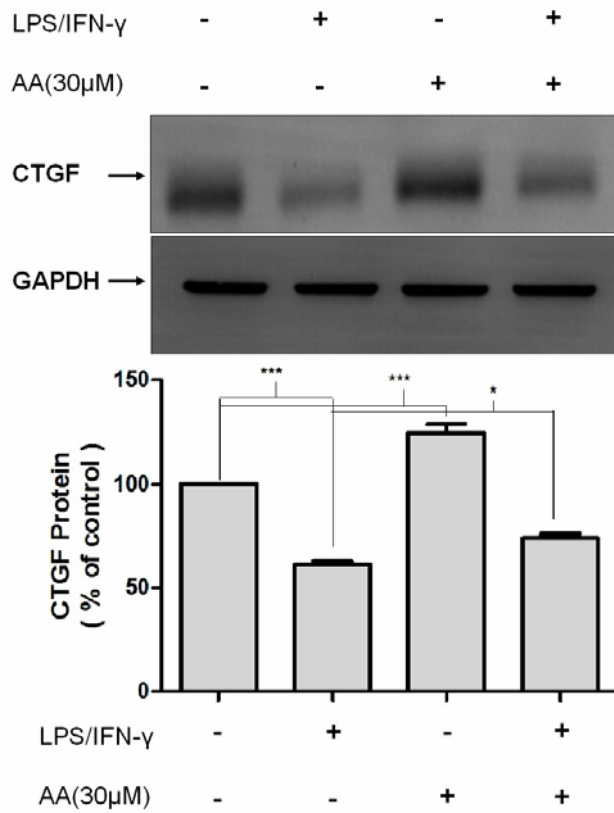


Fig. 1 (A)

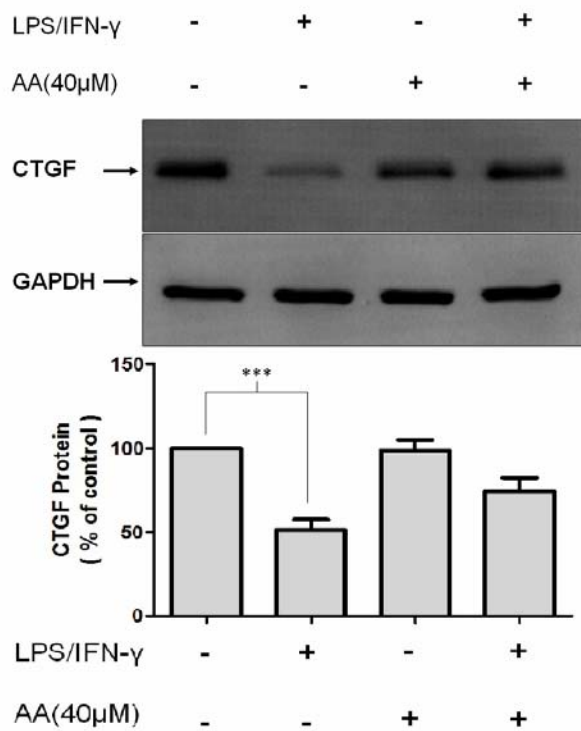


Fig. 1 (B)

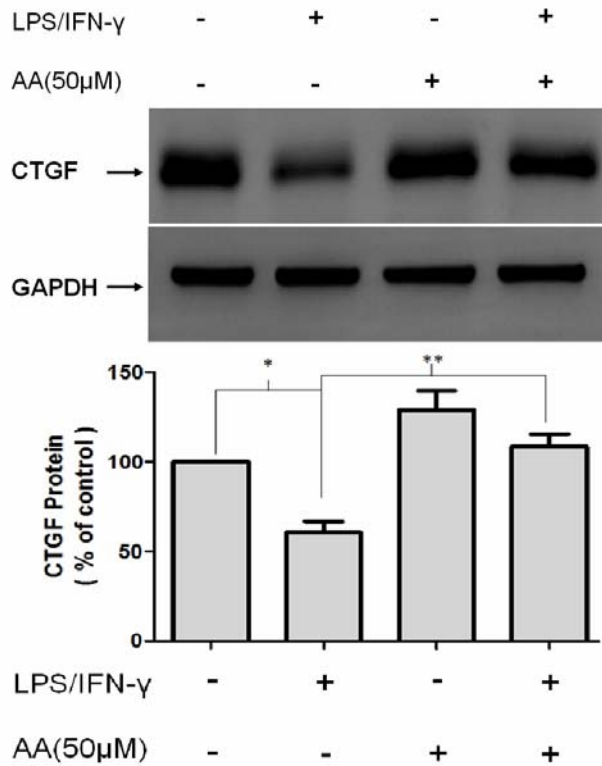
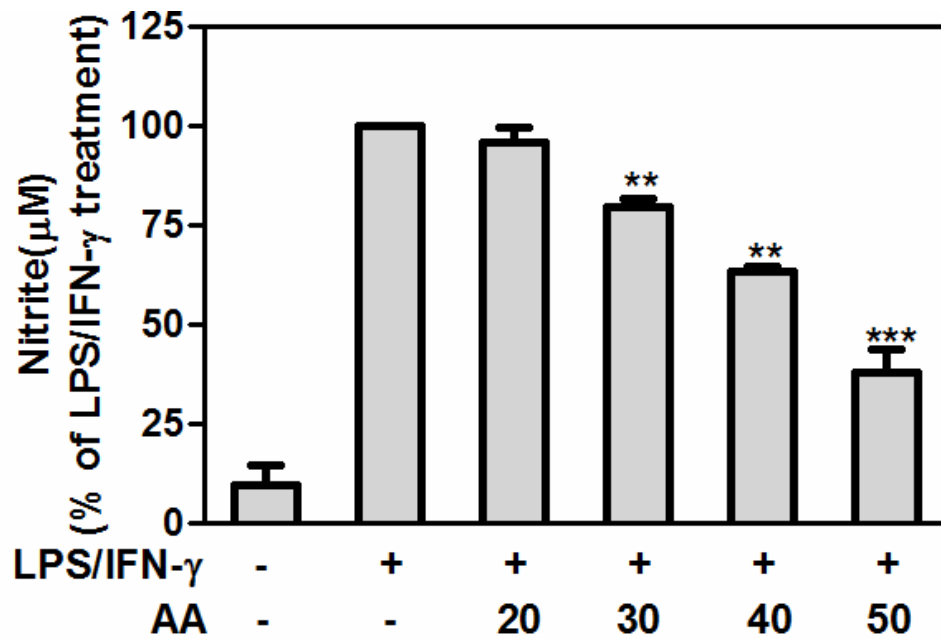


Fig. 1 (C)

**Fig. 1. NO endogenously generated by the induction of iNOS with LPS/IFN- $\gamma$  significantly downregulated the protein expression of CTGF in AA-treated MES-13 cells.** Cells were treated for 24 h with medium only (lane 1: control) or a mixture of 1  $\mu$ g/ml lipopolysaccharide (LPS) and 10 ng/ml interferon (IFN)- $\gamma$  in the absence of various concentrations of AA (lane 2) or presence of various concentrations of AA (lane 4). Cells were also treated with AA only (lane 3). Treatment of AA at concentrations of 30  $\mu$ M, 40 $\mu$ M, and 50  $\mu$ M are shown in (A), (B) and (C), respectively. CTGF protein expressions were determined by Western blot analysis. GAPDH was used as an internal control. Relative protein levels were quantified by scanning densitometry and are expressed as a percentage of the maximal band intensity of the CTGF protein from control cultures. Data represent the mean  $\pm$  SEM of CTGF / GAPDH from at least three separate experiments, and asterisks indicate a significant difference from control (\*  $p$ <0.05, \*\*  $p$ <0.01, \*\*\*  $p$ <0.001).





**Fig. 2. Effect of AA on lipopolysaccharide (LPS)/interferon (IFN)- $\gamma$ -stimulated nitrite synthesis in MES-13 cells.** Cells were treated for 24 h with a mixture of 1  $\mu$ g/ml LPS and 10 ng/ml IFN- $\gamma$  in the absence or presence of various concentrations of AA. Nitrite levels were measured by the Griess reaction. Data are the mean  $\pm$ SEM of at least three separate experiments and are expressed as the percentage of the culture treated with LPS/IFN- $\gamma$  alone. Asterisks indicate a significant difference from treatment with LPS/IFN- $\gamma$  alone (\*\*  $p$ <0.01, \*\*\*  $p$ <0.001).

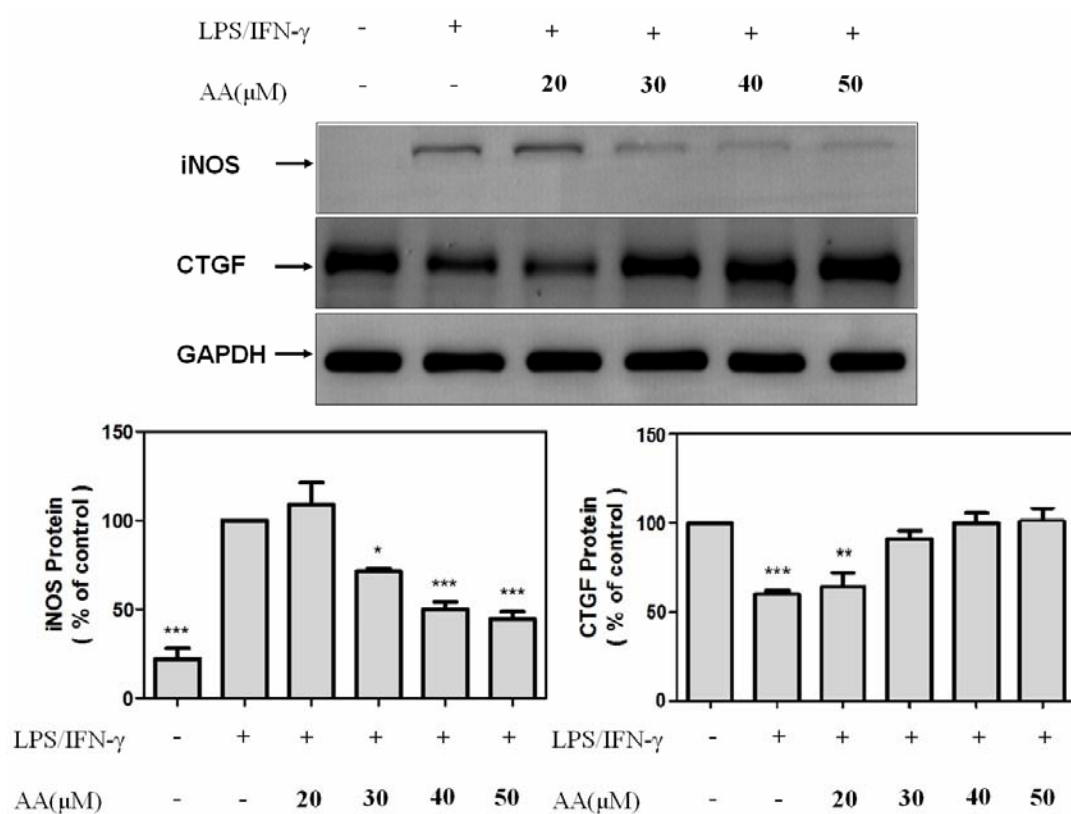
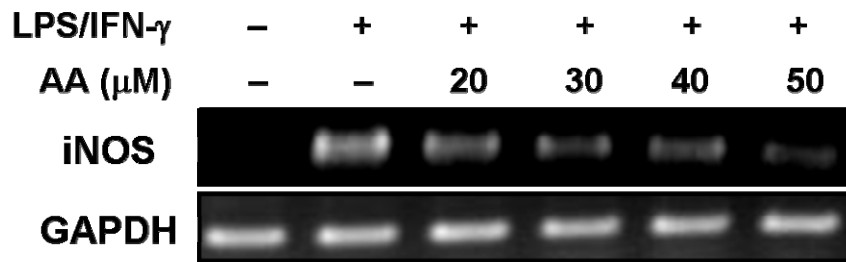


**Fig. 3. Effect of AA on lipopolysaccharide (LPS)/interferon (IFN)- $\gamma$ -stimulated iNOS and CTGF protein expression in MES-13 cells.** Cells were treated for 24 h with a mixture of 1  $\mu$ g/ml LPS and 10 ng/ml IFN- $\gamma$  in the absence or presence of various concentrations of AA. iNOS and CTGF protein expressions were determined by Western blot analysis. GAPDH was used as an internal control. Relative protein levels were quantified by scanning densitometry and are expressed as a percentage of the maximal band intensity of the iNOS protein from cultures treated with LPS/IFN- $\gamma$  alone. For quantification of CTGF protein expression, the maximal band intensity of the CTGF protein was determined by control cultures with medium only. Data are the mean  $\pm$ SEM of iNOS/GAPDH from at least three separate experiments, and asterisks indicate a significant difference from treatment with LPS/IFN- $\gamma$  alone (\*  $p$ <0.05, \*\*  $p$ <0.01, \*\*\*  $p$ <0.005).

(A)



(B)

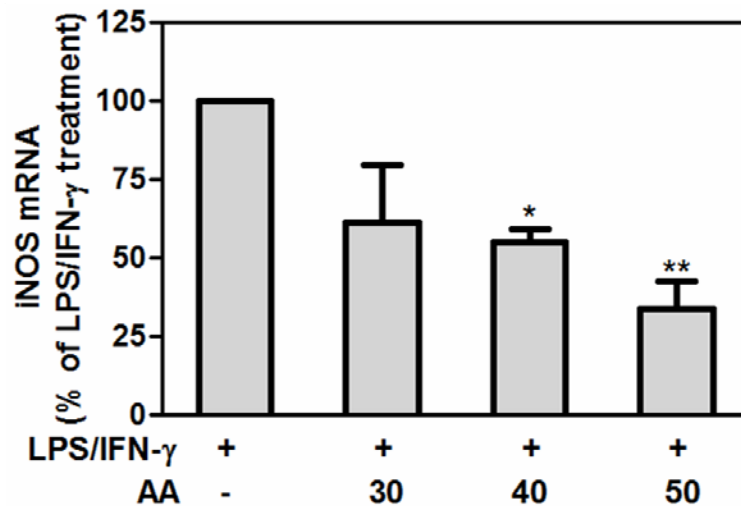


**Fig. 4. Effects of AA on lipopolysaccharide (LPS)/interferon (IFN)- $\gamma$ -stimulated inducible nitric oxide synthase (iNOS) mRNA expression in MES-13 cells assessed by (A) an RT-PCR and (B) real-time RT-PCR.** Cells were treated for 24 h with a mixture of 1  $\mu$ g/ml LPS and 10 ng/ml IFN- $\gamma$  in the absence or presence of various concentrations of AA. mRNA levels of iNOS were measured by an RT-PCR and real-time RT-PCR. GAPDH was used as an internal control. Relative mRNA levels were quantified by scanning densitometry and are expressed as a percentage of the maximal band intensity of iNOS mRNA from cultures treated with LPS/IFN- $\gamma$  alone. Data are the mean  $\pm$ SEM of iNOS/GAPDH of at least three separate experiments, and asterisks indicate a significant difference from the culture treated with LPS/IFN- $\gamma$  alone (\*  $p$ <0.05, \*\*  $p$ <0.01).

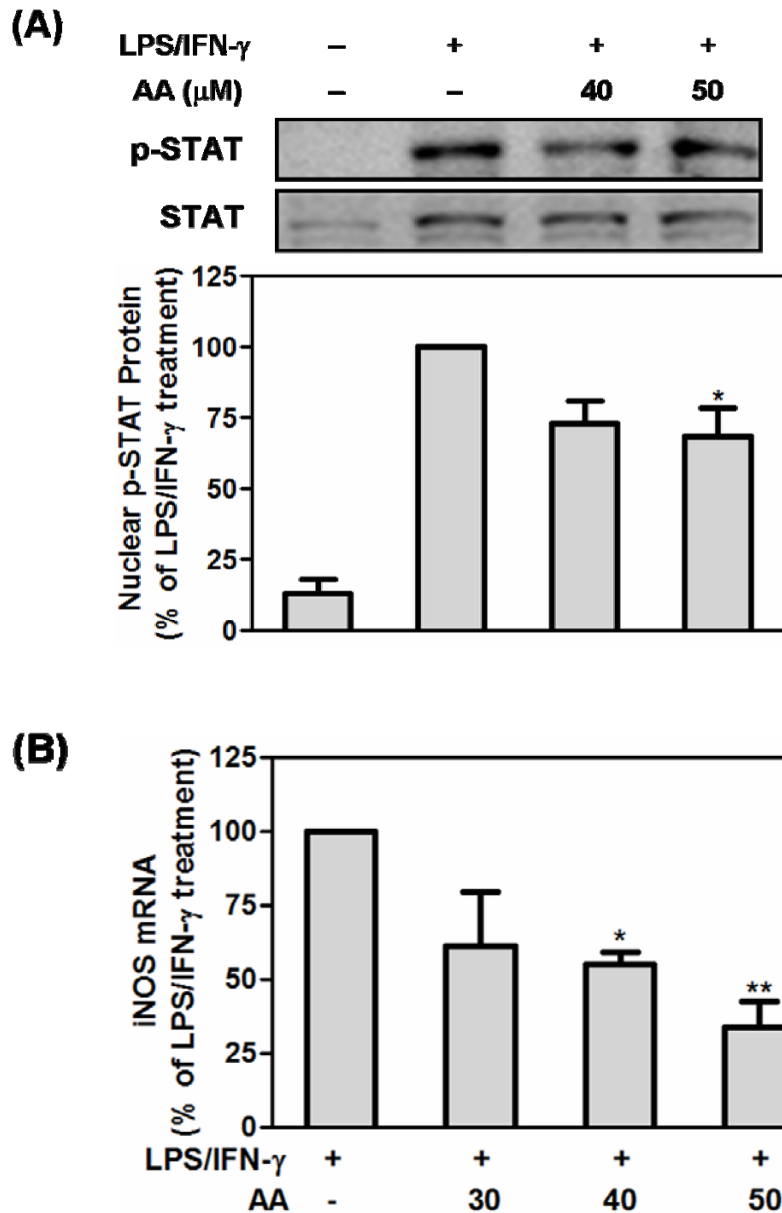


**Fig. 5. Effects of AA on lipopolysaccharide (LPS)/interferon (IFN)- $\gamma$ -stimulated signal transducer and activator of transcription (STAT)-1 $\alpha$  activation and interferon response factor (IRF)-1 protein expressions in MES-13 cells. (A)** Cells were pre-incubated with or without AA for 12 h and then treated in the absence or presence of 1  $\mu$ g/ml LPS and 10 ng/ml IFN- $\gamma$  or 40 min. The nuclear fractions were used to analyze the content of STAT-1 $\alpha$  protein expression and phosphorylated STAT-1 $\alpha$  level by Western blotting. Relative protein levels were quantified by scanning densitometry and are expressed as a percentage of the maximal band intensity in the culture treated with LPS/IFN- $\gamma$  alone. Data are the mean  $\pm$  SEM of phosphorylated STAT-1 $\alpha$ /STAT-1 $\alpha$  protein from at least three separate experiments,

and asterisks indicate significant difference from treatment with LPS/IFN- $\gamma$  alone (\*  $p < 0.05$ ). (B) Cells were treated for 24 h with a mixture of 1  $\mu\text{g/ml}$  LPS and 10  $\text{ng/ml}$  IFN- $\gamma$  in the absence or presence of AA at various concentrations.  $\beta$ -Actin was used as an internal control. Data are the mean  $\pm$ SEM of IRF-1/ $\beta$ -actin from at least three separate experiments and are expressed as a percentage of the culture treated with LPS/IFN- $\gamma$  alone. Asterisks indicate a significant difference from treatment with LPS/IFN- $\gamma$  alone (\*  $p < 0.05$ , \*\*  $p < 0.01$ ).

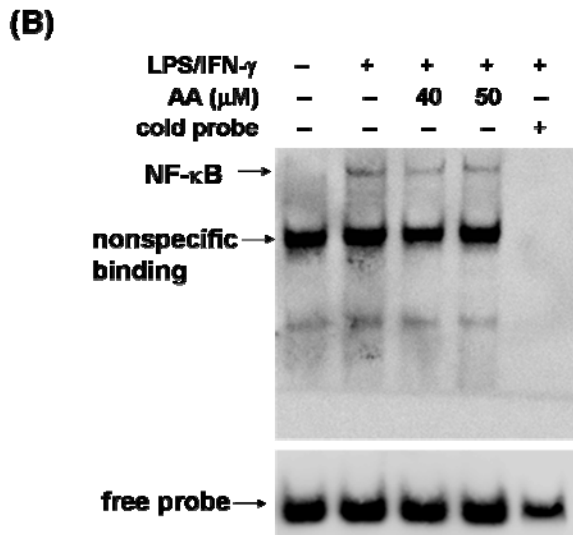
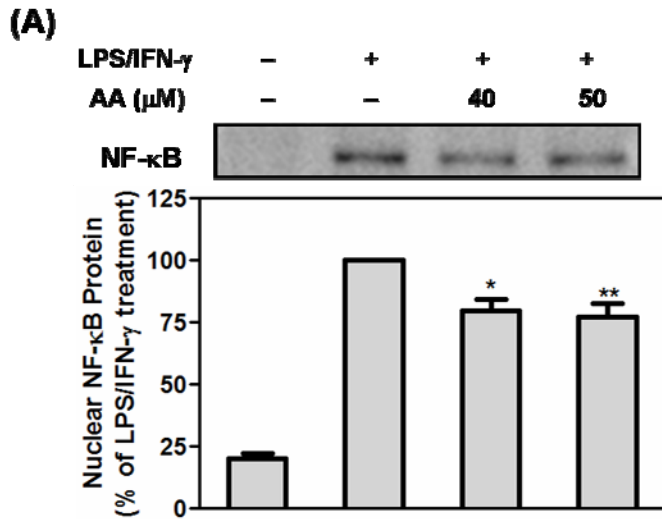


**Fig.6. Effects of AA on lipopolysaccharide (LPS)/interferon (IFN)- $\gamma$ -stimulated nuclear factor (NF)- $\kappa$ B protein level and DNA-binding activity in MES-13 cells.**

(A) Cells were pre-incubated with or without AA for 12 h and then treated in the absence or presence of a mixture of 1  $\mu$ g/ml LPS and 10 ng/ml IFN- $\gamma$  for 40 min. The nuclear fractions were used to analyze the protein content of NF- $\kappa$ B protein by Western blotting. Relative protein levels were quantified by scanning densitometry and are expressed as a percentage of the maximal band intensity in the culture treated with LPS/IFN- $\gamma$  alone. Data are the mean  $\pm$ SEM of at least three separate experiments, and asterisks indicate a significant difference from treatment with LPS/IFN- $\gamma$  alone (\*  $p$ <0.05, \*\*  $p$ <0.01). (B) EMSA experiments of NF- $\kappa$ B DNA-binding activity were carried out using the LightShift Chemiluminescent EMSA Kit from Pierce Chemical. The position of the DNA-protein complex (NF- $\kappa$ B) and the free oligonucleotide are indicated.

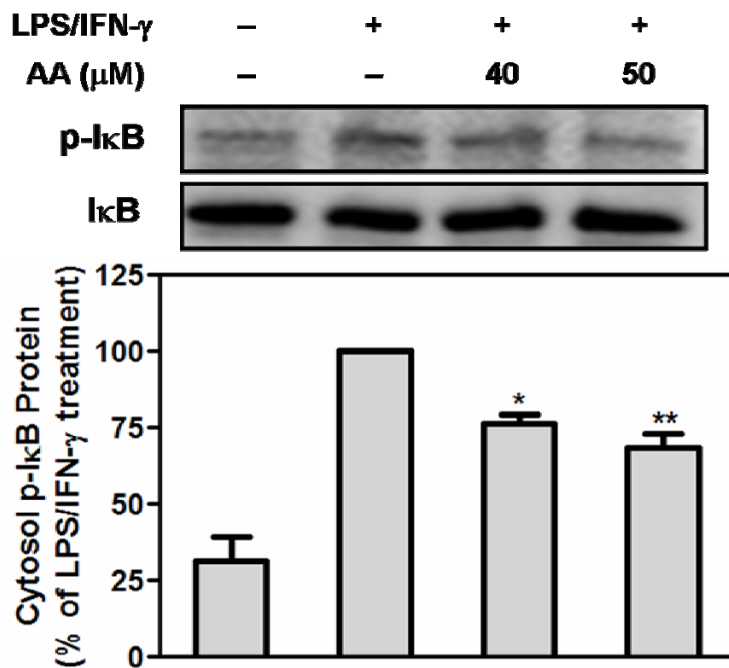


**Fig. 7. Effects of AA on lipopolysaccharide (LPS)/interferon (IFN)- $\gamma$ -stimulated phosphorylated inhibitory factor- $\kappa$ B (I $\kappa$ B)- $\alpha$  protein level and I $\kappa$ B- $\alpha$  protein expression in MES-13 cells.** Cells were pre-incubated with or without AA for 12 h and then treated in the absence or presence of a mixture of 1  $\mu$ g/ml LPS and 10 ng/ml IFN- $\gamma$  for 20 min. The cytosolic fractions were used to analyze the protein content of I $\kappa$ B- $\alpha$  and phosphorylated I $\kappa$ B- $\alpha$  protein by Western blotting. Relative protein levels were quantified by scanning densitometry and are expressed as a percentage of the maximal band intensity in the culture treated with LPS/IFN- $\gamma$  alone. Data are the mean  $\pm$ SEM of at least three separate experiments, and asterisks indicate a significant difference from treatment with LPS/IFN- $\gamma$  alone (\*  $p$ <0.05, \*\*  $p$ <0.01).

## References

- [1] C. Bogdan, Nitric oxide and the immune response, *Nat Immunol* 2 (2001) 907-916.
- [2] F. Aktan, iNOS-mediated nitric oxide production and its regulation, *Life Sci* 75 (2004) 639-653.
- [3] U. Forstermann, W.C. Sessa, Nitric oxide synthases: regulation and function, *Eur Heart J* 33 (2012) 829-837, 837a-837d.
- [4] B.C. Kone, Nitric oxide in renal health and disease, *Am J Kidney Dis* 30 (1997) 311-333.
- [5] H. de Jonge, Y. Vanrenterghem, Aristolochic acid: the common culprit of Chinese herbs nephropathy and Balkan endemic nephropathy, *Nephrol Dial Transplant* 23 (2008) 39-41.
- [6] V.M. Arlt, M. Stiborova, J. vom Brocke, M.L. Simoes, G.M. Lord, J.L. Nortier, M. Hollstein, D.H. Phillips, H.H. Schmeiser, Aristolochic acid mutagenesis: molecular clues to the aetiology of Balkan endemic nephropathy-associated urothelial cancer, *Carcinogenesis* 28 (2007) 2253-2261.
- [7] J.L. Vanherweghem, M. Depierreux, C. Tielemans, D. Abramowicz, M. Dratwa, M. Jadoul, C. Richard, D. Vandervelde, D. Verbeelen, R. Vanhaelen-Fastre, et al., Rapidly progressive interstitial renal fibrosis in young women: association with slimming regimen including Chinese herbs, *Lancet* 341 (1993) 387-391.
- [8] C.S. Yang, C.H. Lin, S.H. Chang, H.C. Hsu, Rapidly progressive fibrosing interstitial nephritis associated with Chinese herbal drugs, *Am J Kidney Dis* 35 (2000) 313-318.
- [8] C.S. Yang, C.H. Lin, S.H. Chang, H.C. Hsu, Rapidly progressive fibrosing interstitial nephritis associated with Chinese herbal drugs, *Am J Kidney Dis* 35 (2000) 313-318.
- [9] I. Cicha, M. Goppelt-Struebe, Connective tissue growth factor: context-dependent functions and mechanisms of regulation, *Biofactors* 35 (2009) 200-208.
- [10] H. Ihn, Pathogenesis of fibrosis: role of TGF-beta and CTGF, *Curr Opin Rheumatol* 14 (2002) 681-685.
- [11] Y. Ito, J. Aten, R.J. Bende, B.S. Oemar, T.J. Rabelink, J.J. Weening, R. Goldschmeding, Expression of connective tissue growth factor in human renal fibrosis, *Kidney Int* 53 (1998) 853-861.



- [12] M. Fragiadaki, A.S. Witherden, T. Kaneko, S. Sonnylal, C.D. Pusey, G. Bou-Gharios, R.M. Mason, Interstitial fibrosis is associated with increased COL1A2 transcription in AA-injured renal tubular epithelial cells in vivo, *Matrix Biol* 30 (2011) 396-403.
- [13] C. Baylis, Nitric oxide deficiency in chronic kidney disease, *Am J Physiol Renal Physiol* 294 (2008) F1-9.
- [14] S. Klahr, The role of nitric oxide in hypertension and renal disease progression, *Nephrol Dial Transplant* 16 Suppl 1 (2001) 60-62.
- [15] C.P. Verdon, B.A. Burton, R.L. Prior, Sample pretreatment with nitrate reductase and glucose-6-phosphate dehydrogenase quantitatively reduces nitrate while avoiding interference by NADP<sup>+</sup> when the Griess reaction is used to assay for nitrite, *Anal Biochem* 224 (1995) 502-508.
- [16] C. Schindler, J.E. Darnell, Jr., Transcriptional responses to polypeptide ligands: the JAK-STAT pathway, *Annu Rev Biochem* 64 (1995) 621-651.
- [17] Q.W. Xie, R. Whisnant, C. Nathan, Promoter of the mouse gene encoding calcium-independent nitric oxide synthase confers inducibility by interferon gamma and bacterial lipopolysaccharide, *J Exp Med* 177 (1993) 1779-1784.
- [18] T. Rein, M. Muller, H. Zorbas, In vivo footprinting of the IRF-1 promoter: inducible occupation of a GAS element next to a persistent structural alteration of the DNA, *Nucleic Acids Res* 22 (1994) 3033-3037.
- [19] H. Kleinert, A. Pautz, K. Linker, P.M. Schwarz, Regulation of the expression of inducible nitric oxide synthase, *Eur J Pharmacol* 500 (2004) 255-266.
- [20] J. Li, Z. Zhang, D. Wang, Y. Wang, Y. Li, G. Wu, TGF-beta 1/Smads signaling stimulates renal interstitial fibrosis in experimental AAN, *J Recept Signal Transduct Res* 29 (2009) 280-285.
- [21] F.D. Debelle, J.L. Nortier, C.P. Husson, E.G. De Prez, A.R. Vienne, K. Rombaut, I.J. Salmon, M.M. Deschodt-Lanckman, J.L. Vanherweghem, The renin-angiotensin system blockade does not prevent renal interstitial fibrosis induced by aristolochic acids, *Kidney Int* 66 (2004) 1815-1825.
- [22] O. Lukivskaya, E. Patsenker, R. Lis, V.U. Buko, Inhibition of inducible nitric oxide synthase activity prevents liver recovery in rat thioacetamide-induced fibrosis reversal, *Eur J Clin Invest* 38 (2008) 317-325.
- [23] F. Mihout, N. Shweke, N. Bige, C. Jouanneau, J.C. Dussaule, P. Ronco, C. Chatziantoniou, J.J. Boffa, Asymmetric dimethylarginine (ADMA) induces chronic kidney disease through a mechanism involving collagen and TGF-beta1 synthesis, *J Pathol* 223 (2011) 37-45.
- [24] H. Kikuchi, T. Katsuramaki, K. Kukita, S. Taketani, M. Meguro, M. Nagayama, M. Isobe, T. Mizuguchi, K. Hirata, New strategy for the

- antifibrotic therapy with oral administration of FR260330 (a selective inducible nitric oxide synthase inhibitor) in rat experimental liver cirrhosis, *Wound Repair Regen* 15 (2007) 881-888.
- [25] M.G. Ferrini, D. Vernet, T.R. Magee, A. Shahed, A. Qian, J. Rajfer, N.F. Gonzalez-Cadavid, Antifibrotic role of inducible nitric oxide synthase, *Nitric Oxide* 6 (2002) 283-294.
- [26] J.J. Morrissey, S. Ishidoya, R. McCracken, S. Klahr, Nitric oxide generation ameliorates the tubulointerstitial fibrosis of obstructive nephropathy, *J Am Soc Nephrol* 7 (1996) 2202-2212.
- [27] D. Hochberg, C.W. Johnson, J. Chen, D. Cohen, J. Stern, E.D. Vaughan, Jr., D. Poppas, D. Felsen, Interstitial fibrosis of unilateral ureteral obstruction is exacerbated in kidneys of mice lacking the gene for inducible nitric oxide synthase, *Lab Invest* 80 (2000) 1721-1728.
- [28] H. Trachtman, S. Futterweit, E. Pine, J. Mann, E. Valderrama, Chronic diabetic nephropathy: role of inducible nitric oxide synthase, *Pediatr Nephrol* 17 (2002) 20-29.
- [29] E. Dreieicher, K.F. Beck, S. Lazaroski, M. Boosen, W. Tsalastra-Greul, M. Beck, I. Fleming, L. Schaefer, J. Pfeilschifter, Nitric oxide inhibits glomerular TGF-beta signaling via SMOC-1, *J Am Soc Nephrol* 20 (2009) 1963-1974.
- [30] A. Keil, I.E. Blom, R. Goldschmeding, H.D. Rupperecht, Nitric oxide down-regulates connective tissue growth factor in rat mesangial cells, *Kidney Int* 62 (2002) 401-411.
- [31] J. Wani, M. Carl, A. Henger, P.J. Nelson, H. Rupperecht, Nitric oxide modulates expression of extracellular matrix genes linked to fibrosis in kidney mesangial cells, *Biol Chem* 388 (2007) 497-506.
- [32] S.H. Sims, Y. Cha, M.F. Romine, P.Q. Gao, K. Gottlieb, A.B. Deisseroth, A novel interferon-inducible domain: structural and functional analysis of the human interferon regulatory factor 1 gene promoter, *Mol Cell Biol* 13 (1993) 690-702.
- [33] S. Vallabhapurapu, M. Karin, Regulation and function of NF-kappaB transcription factors in the immune system, *Annu Rev Immunol* 27 (2009) 693-733.
- [34] Y.Y. Chen, S.Y. Chiang, H.C. Wu, S.T. Kao, C.Y. Hsiang, T.Y. Ho, J.G. Lin, Microarray analysis reveals the inhibition of nuclear factor-kappa B signaling by aristolochic acid in normal human kidney (HK-2) cells, *Acta Pharmacol Sin* 31 (2010) 227-236.

- [35] C.J. Wu, Y.C. Chou, Y.W. Cheng, C.J. Hsiao, C.H. Wang, H.Y. Wang, J.R. Sheu, G. Hsiao, Aristolochic acid downregulates monocytic matrix metalloproteinase-9 by inhibiting nuclear factor-kappaB activation, *Chem Biol Interact* 192 (2011) 209-219.
- [36] M. Vivancos, J.J. Moreno, Role of Ca(2+)-independent phospholipase A(2) and cyclooxygenase/lipoxygenase pathways in the nitric oxide production by murine macrophages stimulated by lipopolysaccharides, *Nitric Oxide* 6 (2002) 255-262.
- [37] M.D. Rosenthal, B.S. Vishwanath, R.C. Franson, Effects of aristolochic acid on phospholipase A2 activity and arachidonate metabolism of human neutrophils, *Biochim Biophys Acta* 1001 (1989) 1-8.
- [38] J.J. Moreno, Effect of aristolochic acid on arachidonic acid cascade and in vivo models of inflammation, *Immunopharmacology* 26 (1993) 1-9.
- [39] Y.S. Lin, M. Hsieh, Y.J. Lee, K.L. Liu, T.H. Lin, AH23848 accelerates inducible nitric oxide synthase degradation through attenuation of cAMP signaling in glomerular mesangial cells, *Nitric Oxide* 18 (2008) 93-104.

# 國科會補助計畫衍生研發成果推廣資料表

日期:2013/10/28

國科會補助計畫	計畫名稱: 探討磷脂酰肌醇三激?抑制劑在 Anti-Thy-1抗體引發腎絲球腎炎動物模式中的抗發炎功能
	計畫主持人: 林庭慧
	計畫編號: 101-2314-B-040-004- 學門領域: 腎臟科新陳代謝及內分泌
無研發成果推廣資料	

101 年度專題研究計畫研究成果彙整表

計畫主持人：林庭慧		計畫編號：101-2314-B-040-004-				計畫名稱：探討磷脂醯肌醇三激?抑制劑在 Anti-Thy-1 抗體引發腎絲球腎炎動物模式中的抗發炎功能	
成果項目		量化			單位	備註（質化說明：如數個計畫共同成果、成果列為該期刊之封面故事...等）	
		實際已達成數（被接受或已發表）	預期總達成數（含實際已達成數）	本計畫實際貢獻百分比			
國內	論文著作	期刊論文	0	0	100%	篇	
		研究報告/技術報告	0	0	100%		
		研討會論文	0	0	100%		
		專書	0	0	100%		
	專利	申請中件數	0	0	100%	件	
		已獲得件數	0	0	100%		
	技術移轉	件數	0	0	100%	件	
		權利金	0	0	100%	千元	
	參與計畫人力（本國籍）	碩士生	0	0	100%	人次	
		博士生	0	0	100%		
		博士後研究員	0	0	100%		
		專任助理	0	0	100%		
國外	論文著作	期刊論文	0	1	60%	篇	
		研究報告/技術報告	0	0	100%		
		研討會論文	0	0	100%		
		專書	0	0	100%	章/本	
	專利	申請中件數	0	0	100%	件	
		已獲得件數	0	0	100%		
	技術移轉	件數	0	0	100%	件	
		權利金	0	0	100%	千元	
	參與計畫人力（外國籍）	碩士生	0	0	100%	人次	
		博士生	0	0	100%		
		博士後研究員	0	0	100%		
		專任助理	0	0	100%		

<p>其他成果 (無法以量化表達之成果如辦理學術活動、獲得獎項、重要國際合作、研究成果國際影響力及其他協助產業技術發展之具體效益事項等，請以文字敘述填列。)</p>	<p>無</p>
--	----------

	成果項目	量化	名稱或內容性質簡述
科 教 處 計 畫 加 填 項 目	測驗工具(含質性與量性)	0	
	課程/模組	0	
	電腦及網路系統或工具	0	
	教材	0	
	舉辦之活動/競賽	0	
	研討會/工作坊	0	
	電子報、網站	0	
	計畫成果推廣之參與(閱聽)人數	0	

# 國科會補助專題研究計畫成果報告自評表

請就研究內容與原計畫相符程度、達成預期目標情況、研究成果之學術或應用價值（簡要敘述成果所代表之意義、價值、影響或進一步發展之可能性）、是否適合在學術期刊發表或申請專利、主要發現或其他有關價值等，作一綜合評估。

## 1. 請就研究內容與原計畫相符程度、達成預期目標情況作一綜合評估

達成目標

未達成目標（請說明，以 100 字為限）

實驗失敗

因故實驗中斷

其他原因

說明：

原本研究計畫所提之實驗設計，其實驗結果不如預期。因此，於計畫執行期中，修改實驗目標。本份成果報告之研究內容與原計畫仍有一定程度相關，即討論一氧化氮及其調控之相關訊息傳遞路徑對腎臟疾病之影響。

## 2. 研究成果在學術期刊發表或申請專利等情形：

論文： 已發表  未發表之文稿  撰寫中  無

專利： 已獲得  申請中  無

技轉： 已技轉  洽談中  無

其他：（以 100 字為限）

## 3. 請依學術成就、技術創新、社會影響等方面，評估研究成果之學術或應用價值（簡要敘述成果所代表之意義、價值、影響或進一步發展之可能性）（以 500 字為限）

一些研究報告指出馬兜鈴酸 Aristolochic acid (AA) 可減弱一個調節免疫反應主要的轉錄因子，NF- $\kappa$ B，之激活。然而，在這些論文中並沒有闡明此發現的生理意義。在這篇報告中，我們發現在腎臟絲球體細胞 MES-13 細胞中，馬兜鈴酸 Aristolochic acid (AA) 可減弱 NF- $\kappa$ B 下游其靶基因之一：誘導型一氧化氮合酶 (iNOS) 之表現。最有趣的是，我們證明，LPS / IFN- $\gamma$  誘導內源性一氧化氮 (Nitric Oxide, NO) 的產生，並可下調結締組織生長因子 connective tissue growth factor (CTGF) 在 MES-13 細胞中之表現。CTGF 是腎臟纖維化之主要指標蛋白質。Aristolochic acid (AA) 顯著抑制由 LPS / IFN- $\gamma$  誘導內源性一氧化氮 (NO) 的產生，並扭轉由一氧化氮 (NO) 下調的 CTGF 表達。我們的結果顯示 Aristolochic acid (AA) 可減弱 NF- $\kappa$ B，下調 iNOS 基因，逆轉由一氧化氮 (NO) 下調的 CTGF 蛋白質表達。這些結果或可部分解釋一些馬兜鈴屬植物導致腎臟纖維化之能力。此份研究報告提供馬兜鈴酸腎病之可能致病機轉及提供馬兜鈴酸腎病之治療策略。